COMMUNICATION

CrossMark
← click for updates

Supramolecular assembly-induced enhanced emission of electrospun nanofibers†

Chih-Chia Cheng,*[a] Yeh-Sheng Wang,[b] Feng-Chih Chang,[b] Duu-Jong Lee,[cd] Li-Chih Yang[b] and Jem-Kun Chen[de]

A nucleobase-assembled supramolecular nanofiber is capable of forming network-like polymeric clusters through complementary hydrogen-bonding interactions. It behaves as an effective chromophore that greatly enhances the light emission efficiency of fluorescent fibers, reaching up to three times higher efficiency than the control samples.

Conjugated polymers are extensively studied as novel functional materials due to their excellent optical and electrical properties associated with an extensive delocalization of π-electrons and conformational restrictions.[1,2] One of the most widely studied conjugated polymers is polythiophene (PT), which possesses a relatively high thermal stability, an easier synthetic process, and greater potential to be modified at the 3- and 4-ring positions of the thiophene heterocycles to fine-tune the polymeric characteristics.[3] PT nanofibers produced by the electrospinning technique have a high specific surface area and large inter-fiber porosity, hence possessing enhanced charge transport, electrical conductivity, field effect mobility, and photoluminescence.[4,5] The unique properties of PT fibers make them suitable for use in photovoltaic cells, organic light-emitting diodes and field effect transistors.[6–9] However, PT nanofibers are difficult to obtain owing to their low molecular weights and rigid unstretchable backbone.[10,11] The results showed lots of beads along with the fibers. To overcome such an obstacle, the PT fibers were blended with high molecular weight polymers in solution to provide sufficient elasticity for electrospinning.[12–15]

[a] Graduate Institute of Applied Science and Technology, National Taiwan University of Science and Technology, Taipei 10607, Taiwan.
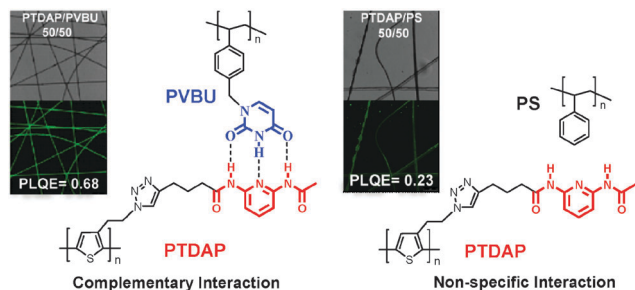E-mail: cccheng@mail.ntust.edu.tw

[b] Institute of Applied Chemistry, National Chiao Tung University, Hsin Chu 30050, Taiwan

[c] Department of Chemical Engineering, National Taiwan University, Taipei 10617, Taiwan

[d] Department of Chemical Engineering, National Taiwan University of Science and Technology, Taipei 10607, Taiwan

[e] Department of Materials Science and Engineering, National Taiwan University of Science and Technology, Taipei 10607, Taiwan

† Electronic supplementary information (ESI) available. See DOI: 10.1039/c4cc07971j

Although conjugated polymer fibers could be electrospun by the incorporation of an auxiliary matrix polymer, the miscibility of a conjugated polymer and a matrix polymer is an important factor affecting the morphology and photophysical properties of conjugated polymer fibers. Xin et al.[16] used a poly(vinyl alcohol)/poly(p-phenylene vinylene) mixture to obtain electrospun fibers and reported a beaded fiber structure. Vohra et al.[9] reported that polyfluorene derivative (F8BT)/polystyrene (PS) blend fibers can be used as active layers of organic light-emitting diodes, but the fluorescence spectra of the nanofiber did not display any polarization dependence. The formation of beads was mainly due to phase separation between the conjugated polymer and the matrix polymer, where occurrence limits further development of electrospinning technology. Controlling the nanofiber structure of conjugated polymers remains challenging. The incorporation of high molecular weight polymers into conjugated polymer matrices is currently quite inefficient when compared to the level of miscible binary polymer pairs in the traditional electrospinning process, which efficiently allows the formation of high-affinity binding networks at the molecular level.[17,18]

Multiple hydrogen-bonding (MHB) interactions have been applied to enhance the miscibility of two immiscible polymers.[19–22] We speculated that introducing MHB into the conjugated polymer and the matrix polymer for electrospinning uniform conjugated polymer nanofibers may considerably affect their phase behavior and provide promising applications as optoelectronic polymer materials.[23] To the best of our knowledge, conjugated polymer nanofibers based on strong hydrogen bonding interaction for tuning the miscibility of the conjugated polymer with the matrix polymer and their photophysical properties have not been previously reported. In this study, a new π-conjugated poly(3-thiophene) containing pendant diamidopyridine group (PTDAP) has been successfully synthesized. PTDAP is expected to interact with its complementary poly1-(4-vinylbenzyl uracil) (PVBU) to form physically cross-linked structures of the complementary uracil–diaminopyridine (U–DAP) pair (Scheme 1).[24,25] As the mechanism of electrospun fiber formation is largely dependent on the viscosity, our materials can be easily used to prepare nanofibers through

Scheme 1 Structural representation of hydrogen-bonding interactions between PTDAP–PVBU and PTDAP–PS systems. Fluorescent photographs of fibers were taken under UV illumination.

complementary hydrogen-bonding interactions and to improve the nanostructure stability and photophysical properties of these systems. This new approach is proposed for the development of next-generation soft matter based on nanofiber and electrospinning technology.

The uracil-functionalized PVBU with high-molecular-weight ($M_w > 250\,550$ g mol^{-1}) was developed.[17] The synthesis of the DAP-functionalized thiophene monomer is described in ESI† (Scheme S1) which was subjected to oxidative polymerization in the presence of iron(III) chloride[26] allowing the preparation of low-regioregular PT containing pendant DAP groups. PTDAP was recovered in high yield (75%), with the resulting PTDAP exhibiting acceptable molecular weight ($M_w = 21\,000$ g mol^{-1}) and polydispersity index (PDI = 1.734), as determined by GPC. However, the PTDAP electrospun fiber is not easily made, due to its low molecular weight leading to jet breakage in the electrospinning process.[11] Therefore, PTDAP is mixed with a high molecular weight PVBU that can be facilely electrospun into uniform fibers at different concentrations. PTDAP is expected to interact with its complementary PVBU to form self-assembled miscible structures of the complementary U–DAP pair (Scheme 1). The FE-SEM images of the resulting PTDAP–PVBU fibers are shown in Fig. 1a. Among the five tested composites of PTDAP–PVBU, the most uniformly distributed fibers with the narrowest

Fig. 1 FE-SEM images of (a) PTDAP–PVBU and (b) PTDAP–PS blend fibers with PTDAP content 1, 5, 10, 25, 50 wt% and their corresponding average diameters.

diameter without beaded structures were obtained. The gradual increase in the average diameters of the fiber with the increasing fraction of PTDAP can be performed to produce uniform fiber structures throughout its growth. In other words, the highly complementary hydrogen bonding was present within the PTDAP–PVBU complex and results in increase in higher viscoelastic forces, thus improving compatibility between PTDAP and PVBU.

In order to compare with the PTDAP–PVBU complex, we blended high molecular weight PS ($M_w = 280\,000$ g mol^{-1}, PDI = 2.87) to prepare electrospun fibers. Fig. 1b shows the FE-SEM images of PTDAP–PS blend fibers with different PTDAP contents. The diameter of the fiber was increased with the PTDAP concentration, from around 0.87 μm to 2.24 μm. However, irregularly shaped fibers with rough surface were obtained, indicating that a low miscibility (Coulombic force) was insufficient to form a continuous fiber. When the composition of PTDAP was increased to 25%, a lot of beads among fibers were formed (Fig. 1b). Further increasing the PTDAP content to 50% results in an immediate increase in the bead number and eventually leading to the formation of bigger beads. As expected, because of their polarity and non-specific interactions, PTDAPs tend to self-aggregate, resulting in an inhomogeneous aggregation in polymer matrices (Scheme 1). Compared to both PVBU–PTDAP and PS–PTDAP blend fibers, the PTDAP–PVBU interaction occurs through strong cooperative hydrogen bonding between PTDAP and PVBU, resulting in highly cross-linked conformational forms in the bulk, even though the structural incompatibilities are present between the chain segments of PS and polythiophene.

The confocal laser scanning microscopy (CLSM) and differential scanning calorimetry (DSC) characterized phase diagrams of the PTDAP–PVBU and PTDAP–PS fibers are shown in Fig. 2a and Fig. S4, ESI.† Each of the PTDAP–PVBU complexes exhibit a continuous fiber structure and uniform fluorescence, indicating that PTDAP is homogeneously dispersed in the PVBU matrix (Fig. 2a). Conversely, the PTDAP–PS blend fibers reveal that bead and discontinuous fibers were spun from 10 to 50 wt% composites of PTDAP. This observation indicates that the PTDAP–PVBU fibers with strong hydrogen bonding interaction induced the orientation of PTDAP chains along the axis of the fiber, which prevents the aggregation of PTDAP in the electrospinning process and yields a homogeneous fiber. The glass transition temperature (T_g) values of 140 and 199 °C were observed for PTDAP and PVBU, respectively (Fig. S4, ESI†). For all complexes formed, the addition of PTDAP into the PVBU fiber led to an apparent single T_g, whereas control PTDAP–PS fibers exhibit two distinct T_g corresponding to the PTDAP-rich and PS-rich phases, respectively. This result also demonstrates the critical importance of the presence of complementary groups that can strongly improve the miscibility of PTDAP–PVBU through specific hydrogen-bonding interaction. The intermolecular fixing effect from U–DAP interactions is responsible for the observed phase stability improvement during the electrospinning process. Thus, the effect of complementary interaction on the phase transition of the electrospun conjugated polymer nanofiber is intriguing and rarely observed in the past studies. This leads us to further investigate the microstructures of these complexes in the film state using CLSM characterization.
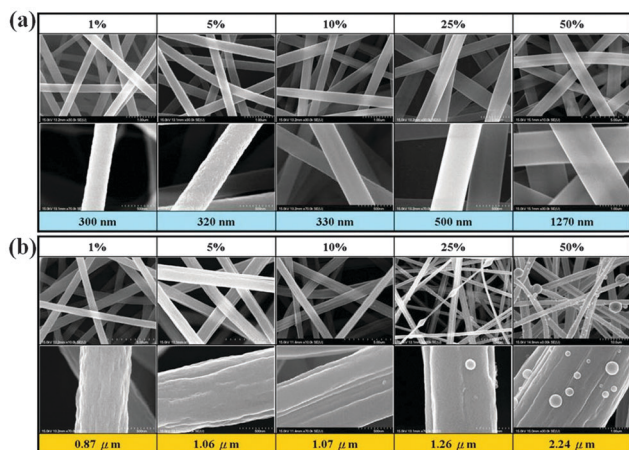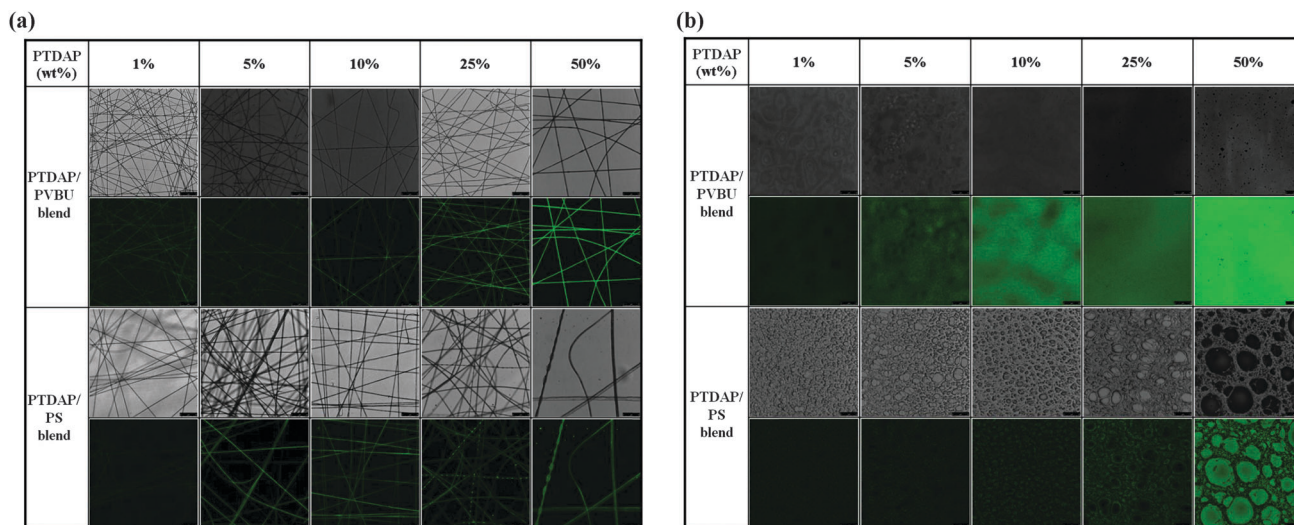
Fig. 2 Optical microscope images and laser confocal microscopic images of PTDAP–PVBU and PTDAP–PS composites with varying PTDAP contents in (a) electrospun fiber and (b) spin-coated film states (the inset scale bar is 25 μm).

In order to understand further the behavior of hydrogen-boning-induced phase transitions, fluorescence images of PTDAP–PVBU and PTDAP–PS thin films were investigated through the measurement of CLSM, and the results are summarized in Fig. 2b. Each set of PTDAP–PVBU composites was homogeneous and uniform fluorescence. In contrast, all composites of PTDAP–PS films present inhomogeneous surfaces and fluorescent islands. The aggregated domain sizes of PTDAP–PS films were increased gradually from 2.67 μm to 26.38 μm with increasing PTDAP content. The phase separation behavior of PTDAP–PS films was significantly greater than those on the corresponding PTDAP–PS nanofibers prepared by electrospinning, being attributable to the more extended PTDAP chain conformation along the fiber axis to reduce the aggregation propensity of PTDAP in comparison with the spin-coated films. However, the thin film of PTDAP–PVBU appears to have the potential to be used in improving the spinnability of conjugated polymers through simple blending, by the specific interaction between complementary U–DAP base pairs. Thus, the U–DAP interaction facilitates the formation of functional nanofiber structures.

To characterize the optical properties of these materials in thin film and fiber states, solid state UV-Vis absorption spectroscopy was employed and results are summarized in Table 1 and Fig. S5 (ESI†). PTDAP–PVBU and PTDAP–PS systems in the fiber state exhibit strong red shift in their UV-Vis spectra. The wavelengths of maximum absorption tended to increase with increasing wt% of PTDAP in both kinds (with PVBU or PS) of electrospun fibers and spin-coated films showed red shift in absorption (Table 1). This observation is due to the uniaxial alignment of the polymer chains with enhancement of the π–π stacking[27] that tends to increase the inter-chain exciton and the aggregation of the chromophoric backbones by applying the electric field during electrospinning. The high stability of the hydrogen bond network can work with the hydrophobic clusters

Table 1 Photophysical properties of PTDAP–PVBU and PTDAP–PS composites

Composition[a]	A_{max}[b] (nm)		PL_{max}[c]		PLQE[d]	
PTDAP/PVBU (weight ratio)	Spin-coated film	Electrospun fiber	Spin-coated film	Electrospun fiber	Spin-coated film	Electrospun fiber
1/99	410	450	535	533	0.04	0.05
5/95	416	451	540	536	0.18	0.21
10/90	418	453	545	545	0.32	0.43
25/75	424	455	556	548	0.43	0.56
50/50	434	455	562	550	0.53	0.68

Composition[a]	A_{max}[b] (nm)		PL_{max}[c]		PLQE[d]	
PTDAP/PSU (weight ratio)	Spin-coated film	Electrospun fiber	Spin-coated film	Electrospun fiber	Spin-coated film	Electrospun fiber
1/99	415	453	543	538	0.04	0.03
5/95	418	454	553	559	0.09	0.12
10/90	418	450	556	558	0.14	0.18
25/75	419	455	557	563	0.19	0.22
50/50	426	461	562	564	0.21	0.23

[a] The weight ratio of PTDAP/matrix polymers. [b] Maximum absorption peak. [c] Maximum emission peak. [d] Photoluminescence quantum yield was determined using a calibrated integrating sphere.

to resist the conformational changes, resulting in a large "confined space".[28] Conversely, for traditional polymers, conjugated chains intermix within a single-phase polymer network to increase the probability of interchain overlap. Fig. S6 and S7 (ESI†) display the photoluminescent (PL) spectra of PTDAP–PVBU and PTDAP–PS composites in fibers and films, respectively. The PL intensities of PTDAP–PVBU blend fibers are substantially increased by introducing PVBU, with the emission wavelengths being significantly blue-shifted compared with PTDAP–PS films. This observation shows that the physically cross-linked network structure through strong cooperative hydrogen bonding reduces the extent of aggregation of the PTDAP chains. According to the above PL results, we anticipated that incorporation of PVBU into PTDAP, which contains chromophoric polythiophene segments, would exhibit improved PL quantum efficiency (PLQE) of its thiophene units. The PLQE of the 5/95 PTDAP/PVBU fiber is 0.21, which is substantially higher than that of the 5/95 PTDAP/PS fiber (PLQE = 0.12) (Table 1). Further increasing the PTDAP content to 50 wt% resulted in the increase in the PLQE value to 0.68, whereas the emission quantum yield of the 50/50 PTDAP/PS fiber is only slightly increased to 0.23 (Scheme 1). These results further demonstrated that incorporation of PVBU into PTDAP significantly influences the photophysical properties of the luminescent electrospun fiber due to the existence of the physically cross-linked structure. Therefore, the enhanced PLQE performance can also be attributed to the phase miscibility and space confinement effect within the electrospun nanofiber. In addition, the photoluminescence behavior of PTDAP–PVBU spin-coated thin films also shows a similar trend to the fiber system, the PLQE of 50/50 PTDAP/PVBU film (PLQE = 0.53) is higher than the PLQE of PTDAP/PS (PLQE = 0.22) (Table 1).

In summary, a new supramolecular light-emitting material has been developed through incorporation of a triple hydrogen bonding array between PTDAP and PVBU as a photoluminescent material. The physically cross-linked PTDAP–PVBU exhibits supreme thermal stability and phase miscibility, a result of the increased cross-link density of the polymer chains. Thus, the continuous bead-free fiber can be fabricated through electrospinning by varying the component ratio of the complex. The photoluminescence measurements illustrated that the hydrogen-bonding networks effectively suppressed aggregation and enhanced the color stability of PTDAP segments in the fiber state. In addition, the resulting fluorescence efficiency of the 50/50 PTDAP/PVBU fiber had reached a maximum value of 0.68, three times higher than those of control PTDAP–PS fibers. The present PTDAP–PVBU system is the first discussion attempting to construct supramolecular pairs in the electrospun fiber as a means of manipulating the photophysical propensities of conjugated polymers

and provides a potential route toward the next generation of self-assembled multifunctional electrospun materials.

Notes and references

1 A. Kraft, A. C. Grimsdale and A. B. Holmes, *Angew. Chem., Int. Ed.*, 1998, **37**, 402.
2 F. J. M. Hoeben, P. Jonkheijm, E. W. Meijer and A. P. H. J. Schenning, *Chem. Rev.*, 2005, **105**, 1491.
3 J. Finden, T. K. Kunz, N. R. Branda and M. O. Wolf, *Adv. Mater.*, 2008, **20**, 1998.
4 H. Dong, V. Nyame, A. G. MacDiarmid and W. E. Jones Jr, *J. Polym. Sci., Part B: Polym. Phys.*, 2004, **42**, 3934.
5 Y. Z. Long, M. M. Li, C. Gu, M. Wan, J. L. Duvail, Z. Liu and Z. Fan, *Prog. Polym. Sci.*, 2011, **36**, 1415.
6 T. Kim, J. H. Im, H. S. Choi, S. J. Yang, S. W. Kim and C. R. Park, *J. Mater. Chem.*, 2011, **21**, 14231.
7 H. Liu, J. B. Edel, L. M. Bellan and H. G. Craighead, *Appl. Phys. Lett.*, 2005, **87**, 253106.
8 J.-Y. Chen, C.-C. Kuo, C.-S. Lai, W.-C. Chen and H.-L. Chen, *Macromolecules*, 2011, **44**, 2883.
9 V. Vohra, U. Giovanella, R. Tubino, H. Murata and C. Botta, *ACS Nano*, 2011, **5**, 5572.
10 A. Laforgue and L. Robitaille, *Synth. Met.*, 2008, **158**, 577.
11 S. Lee, G. D. Moon and U. Jeong, *J. Mater. Chem.*, 2009, **19**, 743.
12 P. Wutticharoenmongkol, P. Supaphol, T. Srikhirin, T. Kerdcharoen and T. Osotchan, *J. Polym. Sci., Part B: Polym. Phys.*, 2005, **43**, 1881.
13 A. Bianco, C. Bertarelli, S. Frisk, J. F. Rabolt, M. C. Gallazzi and G. Zerbi, *Synth. Met.*, 2007, **157**, 276.
14 S. Chuangchote, T. Sagawa and S. Yoshikawa, *Jpn. J. Appl. Phys.*, 2008, **47**, 787.
15 C. C. Kuo, C. H. Lin and W. C. Chen, *Macromolecules*, 2007, **40**, 6959.
16 Y. Xin, Z. H. Huang, E. Y. Yan, W. Zhang and Q. Zhao, *Appl. Phys. Lett.*, 2006, **89**, 053101.
17 Y. S. Wang, C. C. Cheng, Y. S. Ye, Y. C. Yen and F. C. Chang, *ACS Macro Lett.*, 2012, **1**, 159.
18 Y. S. Wang, C. C. Cheng, J. K. Chen, F.-H. Ko and F. C. Chang, *J. Mater. Chem. A*, 2013, **1**, 7745.
19 C. Qin, A. T. N. Pires and L. A. Belfiore, *Macromolecules*, 1991, **24**, 666.
20 H. Zhou, M. L. Xiang, W. J. Chen and M. Jiang, *Macromol. Chem. Phys.*, 1997, **198**, 809.
21 T. Park and S. C. Zimmerman, *J. Am. Chem. Soc.*, 2006, **128**, 11582.
22 I. H. Lin, C. C. Cheng, Y. C. Yen and F. C. Chang, *Macromolecules*, 2010, **43**, 1245.
23 T. Aida, E. W. Meijer and S. I. Stupp, *Science*, 2012, **335**, 813.
24 J. H. Wang, C. C. Cheng, Y. C. Yen, C. C. Miao and F. C. Chang, *Soft Matter*, 2012, **8**, 3747.
25 Y.-L. Chu, C.-C. Cheng, Y. P. Chen, Y. C. Yen and F. C. Chang, *J. Mater. Chem.*, 2012, **22**, 9285.
26 M. Leclerc, F. M. Diaz and G. Wegner, *Makromol. Chem.*, 1989, **190**, 3105.
27 A. Camposeo, I. Greenfeld, F. Tantussi, S. Pagliara, M. Moffa, F. Fuso, M. Allegrini, E. Zussman and D. Pisignano, *Nano Lett.*, 2013, **13**, 5056.
28 (*a*) X. Zhang, Z. Chi, H. Li, B. Xu, X. Li, W. Zhou, S. Liu, Y. Zhang and J. Xu, *Chem. – Asian J.*, 2011, **6**, 808; (*b*) X. Zhang, Z. Chi, J. Zhang, H. Li, B. Xu, X. Li, S. Liu, Y. Zhang and J. Xu, *J. Phys. Chem. B*, 2011, **115**, 7606; (*c*) X. Zhang, Z. Chi, H. Li, B. Xu, X. Li, S. Liu, Y. Zhang and J. R. Xu, *J. Mater. Chem.*, 2011, **21**, 1788.